

Association between Long-term Exposure to Ambient Air Pollution and Myocardial Fibrosis Assessed with Cardiac MRI

Jacques Du Plessis, MD^{1,2} • Chloe DesRoche, MD, MSc³ • Scott Delaney, ScD, JD, MPH⁴ • Rachel C. Nethery, PhD⁵ • Rachel Hong, BSc¹ • Paaladinesh Thavendiranathan, MD, SM^{1,2,6,7} • Heather Ross, MD, MHSc⁶ • Felipe Castillo, MD^{1,2} • Kate Hammeman, MD, MPH^{1,2,7}

Author affiliations, funding, and conflicts of interest are listed at the end of this article.

See also the editorial by Vigneault in this issue.

Radiology 2025; 316(1):e250331 • <https://doi.org/10.1148/radiol.250331> • Content codes: **CA** **MR**

Background: Poor air quality is associated with cardiovascular morbidity. However, the underlying pathophysiologic mechanisms are unclear.

Purpose: To determine the relationship between long-term exposure to ambient fine particulate matter with 2.5- μm or smaller aerodynamic diameter ($\text{PM}_{2.5}$) and the extent of diffuse myocardial fibrosis quantified with cardiac MRI.

Materials and Methods: In this single-center retrospective study, patients with dilated cardiomyopathy (DCM) or controls with normal cardiac MRI findings were included (January 2018 to December 2022). Diffuse myocardial fibrosis was quantified using cardiac MRI native T1 mapping z scores. Residence-specific ambient $\text{PM}_{2.5}$ concentration was assessed as the mean of daily exposure concentration in the year before cardiac MRI using direct measurements from the nearest monitoring station. Multivariable models were adjusted for clinically relevant covariates.

Results: A total of 694 patients (mean age, 47 years \pm 16 [SD]; 443 men; 493 with DCM, 201 controls) were included. In multivariable models, each 1- $\mu\text{g}/\text{m}^3$ increase in 1-year mean $\text{PM}_{2.5}$ exposure was associated with a 0.30 higher native T1 z score in patients with DCM (adjusted β coefficient: 0.30; 95% CI: 0.13, 0.47; $P < .001$) and 0.27 higher native T1 z score in controls (adjusted β coefficient: 0.27; 95% CI: 0.04, 0.51; $P = .02$). For absolute values, each 1- $\mu\text{g}/\text{m}^3$ increase in 1-year mean $\text{PM}_{2.5}$ exposure was associated with 9.1 msec higher native T1 at 1.5 T (β coefficient: 9.1; 95% CI: 2.04, 15.97; $P = .01$) and 12.1 msec higher native T1 at 3 T (β coefficient: 12.1; 95% CI: 5.74, 18.52; $P < .001$). Stratified models indicated the largest effect sizes for the association of $\text{PM}_{2.5}$ exposure with native T1 z scores in women (β coefficient: 0.49; 95% CI: 0.23, 0.76; $P < .001$), smokers (β coefficient: 0.43; 95% CI: 0.02, 0.84; $P = .04$), and patients with hypertension (β coefficient: 0.48; 95% CI: 0.16, 0.80; $P = .004$).

Conclusion: Higher long-term exposure to ambient fine particulate air pollution is associated with greater diffuse myocardial fibrosis at cardiac MRI native T1 mapping in patients with DCM and healthy controls.

© RSNA, 2025

Air pollution is the leading environmental health hazard contributing to excess morbidity and mortality (1). Burning fossil fuels, wildfire smoke, and other human activities release harmful pollutants into the atmosphere (2). Climate change and air pollution are interconnected because air pollutants are frequently co-emitted with greenhouse gases (2–5). Exposure to air pollution is ubiquitous. In 2019, 99% of the world's population lived in places where World Health Organization air quality guideline levels were not met (6). The global cost of health damages associated with exposure to air pollution is estimated at \$8.1 trillion, equivalent to 6.1% of the global gross domestic product (7).

Fine particulate matter with 2.5- μm or smaller aerodynamic diameter ($\text{PM}_{2.5}$) is the most thoroughly studied component of air pollution. $\text{PM}_{2.5}$ is associated with an increased risk of cardiovascular diseases—including myocardial infarction, heart failure, and stroke—and promotes the development of cardiovascular risk factors such as hypertension and diabetes (8,9). The World Health Organization estimates that 31% of cardiovascular disease is attributable to environmental factors—of which air pollution is the most important—accounting for 119 million disability-adjusted life years (10). Nearly 70% of the 4.2 million deaths attributed to ambient air pollution in 2019 were caused by cardiovascular conditions (11). However, the underlying pathophysiologic mechanisms by which exposure

to $\text{PM}_{2.5}$ leads to adverse cardiovascular outcomes are unclear. Hypothesized mechanisms include oxidative stress, inflammation, and autonomic stimulation, potentially leading to activation of cardiac fibroblasts and increased extracellular matrix protein deposition (8,12).

Given its role in maladaptive left ventricular remodeling, myocardial fibrosis could potentially mediate the adverse cardiovascular effects of particulate air pollution and help explain some of the variability in heart failure progression and other adverse cardiac events that are not explained by traditional cardiovascular risk factors (13–15). Myocardial fibrosis is strongly associated with adverse outcomes in many forms of cardiovascular disease, including dilated cardiomyopathy (DCM) (16).

Cardiac MRI allows for noninvasive quantification of diffuse myocardial fibrosis using parametric T1 mapping and assessment of replacement fibrosis using late gadolinium enhancement (LGE) (17–19). While these cardiac MRI markers of fibrosis are associated with adverse cardiovascular outcomes, they have not been used to evaluate myocardial changes associated with air pollution to date (20).

This retrospective study aimed to determine the relationship between long-term exposure to ambient $\text{PM}_{2.5}$ air pollution and the extent of diffuse myocardial fibrosis quantified with cardiac MRI.

Abbreviations

DCM = dilated cardiomyopathy, LGE = late gadolinium enhancement, PM_{2.5} = fine particulate matter with 2.5-µm or smaller aerodynamic diameter

Summary

Higher long-term exposure to ambient fine particulate air pollution is associated with greater diffuse myocardial fibrosis at cardiac MRI native T1 mapping in patients with dilated cardiomyopathy and controls with normal MRI findings.

Key Results

- In a retrospective study of 694 patients, each 1-µg/m³ increase in 1-year mean exposure to ambient fine particulate matter with 2.5-µm or smaller aerodynamic diameter (PM_{2.5}) was associated with a 0.30 higher native T1 z score in patients with dilated cardiomyopathy (adjusted β coefficient: 0.30, P < .001, 493 patients) and 0.27 higher native T1 z score in controls with normal cardiac MRI findings (adjusted β coefficient: 0.27, P = .02, 201 patients) using multivariable models.
- For absolute native T1 values, each 1-µg/m³ increase in 1-year mean PM_{2.5} exposure was associated with 9.1 msec higher native T1 at 1.5 T (β coefficient: 9.1, P = .01) and 12.1 msec higher native T1 at 3 T (β coefficient: 12.1, P < .001).
- In exploratory stratified analyses, effect sizes for the association of ambient PM_{2.5} exposure with native T1 z scores were largest in women (β coefficient: 0.49), smokers (β coefficient: 0.43), and patients with hypertension (β coefficient: 0.48).

Materials and Methods

Study Design

This single-center retrospective study was approved by the institutional ethics committee, and the requirement for written informed consent was waived. Patients were considered eligible

based on the following criteria: referral for cardiac MRI for evaluation of DCM at a large tertiary referral hospital network in Toronto, Canada (University Health Network), between January 2018 and December 2022 with clinical follow-up; age of 18 years or older at the time of cardiac MRI; same residential address for at least 1 year before cardiac MRI; no clinically documented history of congenital heart disease; and no clinical history of myocardial infarction, percutaneous revascularization, or coronary artery bypass grafting. Exclusion criteria included LGE-based evidence of myocardial infarction, as defined by subendocardial pattern LGE in a typical coronary artery distribution; severe valvular

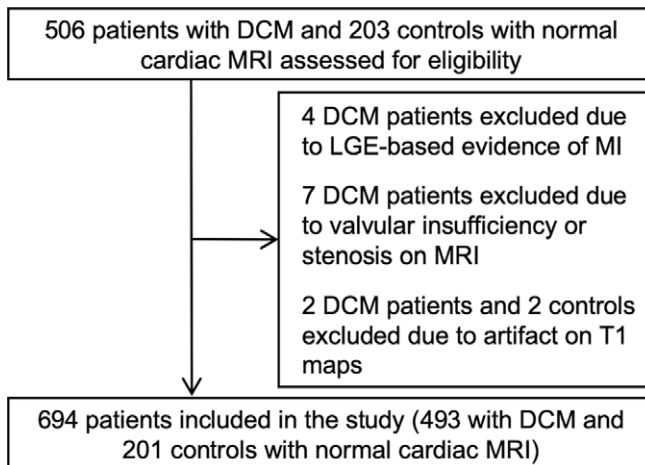


Figure 1: Flowchart details patient selection. An initial 506 eligible patients with dilated cardiomyopathy (DCM) and 203 controls with normal cardiac MRI findings were identified. Fifteen patients were excluded, and a total of 694 patients were included in the final study sample—493 with DCM and 201 controls. LGE = late gadolinium enhancement, MI = myocardial infarction

Table 1: Baseline Patient Characteristics

Characteristic	All Patients (n = 694)	Patients with DCM (n = 493)	Patients with Normal Cardiac MRI Findings (n = 201)
Age (y)*	47 ± 16	48 ± 16	46 ± 16
Male	443 (63.8)	350 (71.0)	93 (46.3)
Female	251 (36.2)	143 (29.0)	108 (53.7)
Height (cm)*	173 ± 14	174 ± 15	170 ± 10
Weight (kg)*	75 ± 17	78 ± 20	75 ± 16
BSA (m ²)*	1.88 ± 0.24	1.92 ± 0.23	1.88 ± 0.23
1-year mean daily ambient PM _{2.5} (µg/m ³) [†]	7.7 (7.2, 8.0)	7.8 (7.4, 8.1)	7.4 (7.0, 7.8)
1-year mean PM _{2.5} exposure below current Canadian ambient air quality standards for annual PM _{2.5}	675 (97.3)	475 (96.4)	200 (99.5)
Ambient temperature on the day of cardiac MRI (°C) [†]	9.4 (1.3, 19.0)	9.4 (2.2, 19.2)	8.5 (1, 18.6)
Distance to nearest station (km) [†]	6.6 (3.7, 10.0)	6.6 (3.5, 9.9)	6.5 (3.8, 10.2)
Urban residence	639 (92.1)	450 (91.3)	189 (94.0)
Hypertension	192 (27.7)	148 (30.0)	44 (21.9)
Hyperlipidemia	123 (17.7)	86 (17.4)	37 (18.4)
Smoking history	68 (9.8)	63 (12.8)	5 (2.5)
Diabetes	69 (9.9)	55 (11.2)	14 (7.0)
Neighborhood median annual household income (\$)†	43 200 (36 800, 50 400)	42 800 (36 800, 50 800)	45 200 (37 600, 50 400)
Neighborhood education level (diploma or higher) (%)*	73 ± 11	73 ± 11	73 ± 10

Note.—Except where indicated, data are numbers of patients or controls, with percentages in parentheses. BSA = body surface area, DCM = dilated cardiomyopathy, PM_{2.5} = fine particulate matter with 2.5-µm or smaller aerodynamic diameter.

* Data are means ± SDs.

† Data are medians, with IQRs in parentheses.

Table 2: Cardiac MRI Findings

Parameter	All Patients (n = 694)	Patients with DCM (n = 493)	Patients with Normal Cardiac MRI Findings (n = 201)
Native T1 z score	0.9 (-0.1, 2.1)	1.4 (0.4, 2.5)	0.0 (-0.7, 0.8)
Native T1 at 1.5 T (msec)*†	1040 ± 52	1054 ± 51	1003 ± 33
Native T1 at 3 T (msec)*†	1254 ± 57	1268 ± 59	1224 ± 38
T2 z score	0.0 (-0.6, 0.7)	0.2 (-0.6, 0.9)	0.0 (-0.7, 0.6)
Native T2 at 1.5 T (msec)*†	46 ± 3	46 ± 3	45 ± 3
Native T2 at 3 T (msec)*†	39 ± 3	39 ± 3	39 ± 3
LVEDVI (mL/m ²)	106 (89, 130)	116 (103, 146)	78 (69, 81)
LVEF (%)	53 (31, 58)	40 (24, 54)	59 (57, 53)
LGE presence‡§	322 (47)	322 (67)	0 (0)

Note.—Except where indicated, data are medians, with IQRs in parentheses. Each patient’s T1 and T2 values were converted to z scores based on scanner-specific T1 and T2 reference values from healthy patients with no evidence of cardiovascular disease (z score = [patient value – mean of scanner-specific normal reference values]/[SD of scanner-specific normal reference values]). By transforming values in this way, z scores provide an assessment of how many SDs each patient’s T1 or T2 value was above or below the mean for the normal range for each scanner. DCM = dilated cardiomyopathy, LGE = late gadolinium enhancement, LVEDVI = left ventricular end-diastolic volume indexed to body surface area, LVEF = left ventricular ejection fraction.

* Cardiac MRI was performed at 1.5 T in 323 patients (239 of 493 patients with DCM and 84 of 201 patients with normal cardiac MRI findings) and at 3 T in 371 patients (254 of 493 patients with DCM and 117 of 201 patients with normal cardiac MRI findings).

† Data are means ± SDs.

‡ Data are numbers of patients or controls, with percentages in parentheses.

§ LGE imaging was available in 683 patients (482 of 493 patients with DCM and 201 of 201 patients with normal cardiac MRI findings); none of the patients with normal cardiac MRI findings had LGE presence as this was one of the criteria to define normal MRI.

Table 3: Univariable and Multivariable Regression for 1-year Mean PM_{2.5} Exposure

Parameter	Univariable Model		Multivariable Model	
	β Coefficient or Odds Ratio	P Value	β Coefficient or Odds Ratio	P Value
All patients (n = 694)				
Native T1 z score*	0.38 (0.24, 0.51)	<.001	0.33 (0.19, 0.48)	<.001
T2 z score*	0.10 (0.01, 0.19)	.03	0.07 (-0.03, 0.17)	.16
LVEDVI (mL/m ²)*	4.7 (1.3, 8.2)	.007	3.6 (0.10, 7.2)	.047
LVEF (%)*	-3.3 (-4.8, -2.0)	<.001	-2.2 (-3.5, -0.80)	.002
LGE presence†	1.4 (1.2, 1.7)	<.001	1.4 (1.1, 1.7)	.005
Patients with DCM (n = 493)				
Native T1 z score*	0.28 (0.13, 0.44)	<.001	0.30 (0.13, 0.47)	<.001
T2 z score*	0.08 (-0.02, 0.18)	.13	0.05 (-0.06, 0.16)	.37
LVEDVI (mL/m ²)*	1.4 (-2.4, 5.2)	.48	2.6 (-1.4, 6.6)	.20
LVEF (%)*	-1.6 (-3.1, -0.3)	.045	-1.2 (-2.8, 0.3)	.11
LGE presence (%)†	1.22 (1.02, 1.47)	.03	1.25 (1.01, 1.56)	.04
Patients with normal MRI findings (n = 201)				
Native T1 z score*	0.21 (0.01, 0.42)	.04	0.27 (0.04, 0.51)	.02
T2 z score*	0.07 (-0.01, 0.17)	.48	0.14 (-0.01, 0.17)	.24
LVEDVI (mL/m ²)*	-1.9 (-5.0, 1.2)	.23	-2.0 (-5.4, 1.3)	.24
LVEF (%)*	-3.6 (-1.1, 0.42)	.36	-0.4 (-1.3, 0.5)	.35
LGE presence (%)†

Note.—Individual multivariable linear and logistic regression models for each MRI parameter (as the dependent variable) and 1-year mean ambient fine particulate matter with 2.5-µm or smaller aerodynamic diameter (PM_{2.5}) exposure (as the independent variable) were adjusted for age, sex, body surface area, local ambient temperature on the day of cardiac MRI, distance in kilometers from residential postal code centroid to nearest air pollution monitoring station, urban versus rural residence location, MRI field strength, year, cardiac risk factors (hypertension, hyperlipidemia, smoking status, and diabetes mellitus), and indicators of socioeconomic status (neighborhood median household income and employment rate by postal code). Each 1-µg/m³ increase in 1-year mean exposure to ambient PM_{2.5} was associated with 0.30 higher native T1 z score in patients with dilated cardiomyopathy (DCM) (adjusted β coefficient: 0.30, P < .001, 493 patients) and 0.27 higher native T1 z score in controls with normal cardiac MRI findings (adjusted β coefficient: 0.27, P = .02, 201 patients) using multivariable models. Numbers in parentheses are 95% CIs. LGE = late gadolinium enhancement, LVEDVI = left ventricular end-diastolic volume indexed to body surface area, LVEF = left ventricular ejection fraction.

* Data are β coefficients and represent the average differences in the magnitude of each MRI parameter (dependent variable) for every 1-µg/m³ increase in 1-year mean ambient PM_{2.5} exposure (independent variable). P values were calculated using linear regression models.

† Data are odds ratios for LGE present on cardiac MRI scans (dependent variable) for every 1-µg/m³ increase in 1-year mean ambient PM_{2.5} exposure (independent variable). P values were calculated using logistic regression models.

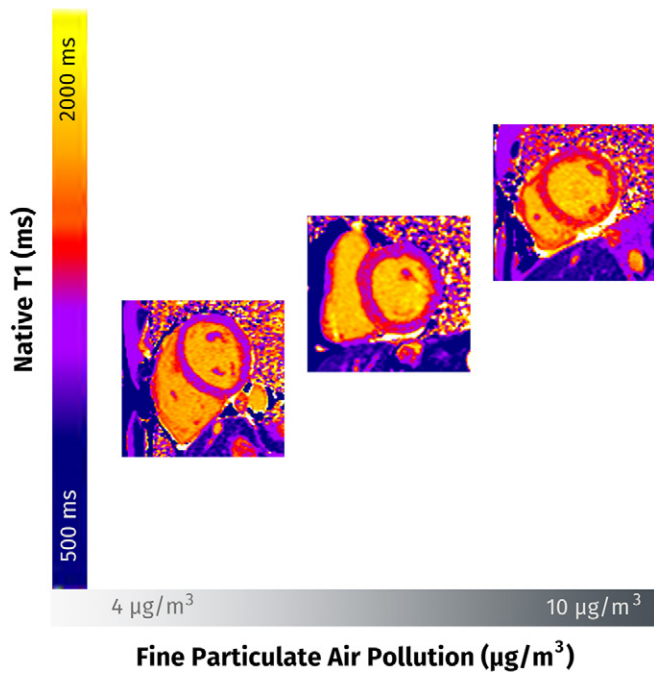


Figure 2: Images from cardiac MRI native T1 mapping show that higher long-term exposure to fine particulate air pollution is associated with higher extent of myocardial fibrosis.

insufficiency or stenosis at MRI; and inability to assess T1 mapping images due to artifact (Fig 1). To contextualize findings in patients without pre-existing cardiovascular disease, we included a control group of adult patients with normal cardiac MRI findings (defined as normal ventricular end-diastolic volumes indexed to body surface area, normal ventricular ejection fraction, normal left ventricular mass and wall thickness, normal atrial size, no LGE, and no significant [more than trace] valve regurgitation) and no adverse cardiac events after a minimum of 1-year follow-up.

Heart failure has multiple underlying causes that impact prognosis, treatment, and cardiac imaging findings. In this study, we specifically focused on patients with nonischemic DCM as a common phenotype in heart failure, which has a poor prognosis despite advances in medical and device therapy (21). Selection of patients with a common underlying cardiovascular disease also minimizes the potential for confounding by other clinical variables.

Cardiac MRI Protocol

Contrast-enhanced cardiac MRI studies were performed using a 1.5- or 3-T scanner (Magnetom AVANTOfit or SKYRAfit; Siemens Healthineers), with both units located in the same hospital with the same catchment area using commercially available cardiac surface coils. The MRI protocol included long-axis sections and a stack of short-axis cine balanced steady-state free precession sections with complete ventricular coverage (section thickness, 8 mm; intersection gap, 2 mm). A single midventricular short-axis T1 and T2 mapping section was acquired using a modified Look-Locker inversion recovery technique for native T1 mapping (5[3]3 inversion grouping) and a matching T2 map was obtained using a T2-preparation technique with read-out varying with external field strength (balanced steady-state free precession at 1.5 T and fast low angle shot at 3 T). Pixel-based T1 and T2 maps

were automatically generated on the scanner with application of inline motion correction algorithms. LGE images were acquired in short- and long-axis views using a two-dimensional phase-sensitive inversion recovery technique starting 12 minutes after intravenous administration of contrast material (0.15 mmol per kilogram body weight gadobutrol; Bayer Healthcare).

Cardiac MRI Analysis

Cardiac MRI studies were analyzed independently by a fellowship-trained radiologist (J.D.P., with 2 years of cardiac MRI expertise) who was blinded to all clinical information using commercially available tools (Circle cmr42; Circle Cardiovascular Imaging). Left ventricular volumes and function were measured using automated contour detection, with manual correction if required. Presence or absence of LGE was evaluated visually. Myocardial T1 and T2 relaxation times were assessed by manually drawing a region of interest at the midinterventricular septum, avoiding the right ventricular insertion points, blood pool, and areas with LGE (17). Given differences in T1 and T2 mapping between scanners and techniques, conversion of z scores can be used to standardize raw values to facilitate combined analysis of data from multiple scanners. Thus, each patient's T1 and T2 values were converted to z scores based on scanner-specific T1 and T2 reference values from healthy patients with no evidence of cardiovascular disease, as follows: (patient value – mean of scanner-specific normal reference values)/(SD of scanner-specific normal reference values) (17,27). By transforming values in this way, z scores could provide an assessment of how many SDs each patient's T1 or T2 value was above or below the mean for the normal range for each scanner.

Outcomes

The primary outcome was myocardial native T1 z score assessed with cardiac MRI. Higher T1 z scores indicate higher extent of diffuse myocardial fibrosis, while lower z scores indicate lower extent of diffuse myocardial fibrosis. Secondary outcomes were myocardial LGE as a marker of myocardial replacement fibrosis (LGE presence is associated with scarring and arrhythmias), left ventricular end-diastolic volume indexed to body surface area as a marker of dilatation (where larger values indicate worse ventricular dilatation), left ventricular ejection fraction as a marker of impaired global systolic function (where lower left ventricular ejection fraction values indicate worse systolic function), and native T2 z score as a marker of myocardial edema (higher T2 z scores indicate higher extent of myocardial edema typically associated with inflammation).

Environmental Exposure

The Government of Ontario Ministry of the Environment, Conservation and Parks has a network of ambient (outside) air monitoring stations across the province that collect real-time air pollution data (22). Using latitude and longitude coordinates, the nearest monitoring station for each patient was determined based on the patient's residential postal code. Long-term $PM_{2.5}$ exposure was calculated for each patient as the mean concentration of daily ambient $PM_{2.5}$ (in micrograms per cubic meters) from the closest monitoring station in the 1-year period immediately before their cardiac MRI examination. Air pollution exposure varies over an individual's life based on geographic location and year. One-year

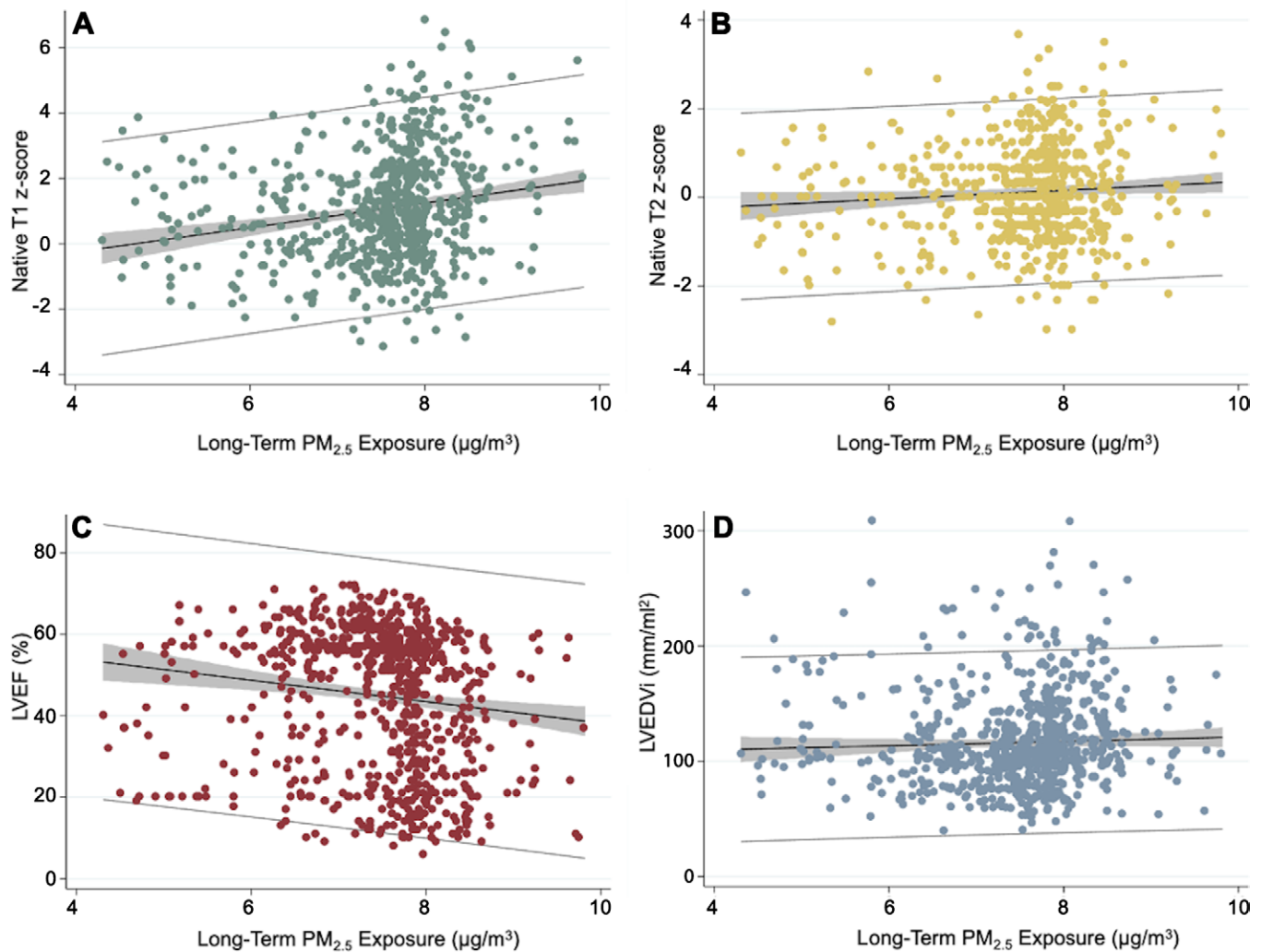


Figure 3: Scatterplots show the relationship between long-term exposure to fine particulate matter with 2.5- μm or smaller aerodynamic diameter ($\text{PM}_{2.5}$) and cardiac MRI parameters in all patients, including **(A)** native T1 z score, **(B)** native T2 z score, **(C)** left ventricular ejection fraction (LVEF), and **(D)** left ventricular end-diastolic volume indexed to body surface area (LVEDVi). Linear regression lines are shown in black, 95% CIs in gray shading, and 95% prediction intervals in blue. Each 1- $\mu\text{g}/\text{m}^3$ increase in 1-year mean ambient $\text{PM}_{2.5}$ exposure was associated with a 0.38 higher native T1 z score (β coefficient: 0.38; 95% CI: 0.24, 0.51; $P < .001$).

mean exposure was selected as an indicator of long-term exposure, similar to other studies, given variability in estimates over longer periods (23,24). Given the potential effects of temperature on $\text{PM}_{2.5}$ and cardiac physiology, the mean ambient 24-hour daily temperature (in degrees Celsius) was also assessed for each patient on the day of their MRI from the closest monitoring station to the hospital where cardiac MRI was performed (25,26).

Statistical Analysis

Statistical analysis was performed using a commercially available software package, STATA, version 14.1 (StataCorp). A two-tailed P value of less than .05 was considered statistically significant. Continuous variables are described using means and SDs or medians and IQRs, and categorical variables are described using numbers and percentages. Linear and logistic regression models were used to investigate the relationship of 1-year mean $\text{PM}_{2.5}$ exposure with individual continuous cardiac MRI parameters and myocardial LGE presence or absence, respectively. The model R^2 indicates how much of the variation in the dependent variable is accounted for by the independent variable. Multi-variable models were adjusted for age, sex, body surface area,

local ambient temperature on the day of cardiac MRI, distance in kilometers from residential postal code centroid to nearest air pollution monitoring station, urban versus rural residence location, MRI scanner (field strength), year, cardiac risk factors (hypertension, hyperlipidemia, smoking status, and diabetes mellitus), and indicators of socioeconomic status (neighborhood median household income and employment rate based on matching individual postal codes to standard Canadian census geographies). Regression model assumptions were assessed using residual plots. In a secondary analysis, the analysis was stratified by patient age (<50 years and ≥ 50 years at the time of cardiac MRI), sex, hypertension, diabetes, smoking status, and MRI unit and field strength. Sensitivity analyses were also performed, using restricted cubic spline transformation of 1-year mean $\text{PM}_{2.5}$ exposure with three knots to investigate nonlinear relationships, restricting the analysis to patients within 10 km and 30 km of the nearest monitoring station, restricting the analysis to MRI performed before 2020 (before COVID-19), and restricting the analysis to patients with 1-year mean $\text{PM}_{2.5}$ exposure below current Canadian Ambient Air Quality Standards (CAAQS) of 8.8 $\mu\text{g}/\text{m}^3$ for annual $\text{PM}_{2.5}$ (28–30).

Table 4: Linear Regression for Native T1 z Score and 1-year Mean PM_{2.5} Exposure in Stratified and Restricted Subgroups

Subgroup	β Coefficient	P Value
Women	0.49 (0.23, 0.76)	<.001
Men	0.26 (0.09, 0.43)	.003
Smoking history	0.43 (0.02, 0.84)	.04
No smoking history	0.33 (0.17, 0.49)	<.001
Hypertension	0.48 (0.16, 0.80)	.004
No hypertension	0.31 (0.15, 0.48)	<.001
Diabetes	0.44 (−0.22, 1.10)	.19
No diabetes	0.32 (0.17, 0.47)	<.001
Patient age <50 years	0.31 (0.12, 0.50)	.001
Patient age ≥50 years	0.29 (0.07, 0.52)	.01
1.5-T scanner*	9.1 (2.04, 15.97)	.01
3-T scanner*	12.1 (5.74, 18.52)	<.001
Within 10 km from an ambient (outside) air monitoring station	0.37 (0.19, 0.56)	<.001
Within 30 km from an ambient (outside) air monitoring station	0.38 (0.22, 0.54)	<.001
MRI performed before the COVID-19 pandemic	0.36 (0.17, 0.55)	<.001
1-year mean PM _{2.5} exposure below current Canadian Ambient Air Quality Standards	0.31 (0.16, 0.46)	<.001

Note.—Effect sizes for the association of ambient fine particulate matter with 2.5-μm or smaller aerodynamic diameter (PM_{2.5}) exposure with native T1 z scores were highest in women (β coefficient: 0.49), smokers (β coefficient: 0.43), and patients with hypertension (β coefficient: 0.48). Except where indicated, the β coefficients represent the average differences in the magnitude of native T1 z score (dependent variable) for every 1-μg/m³ increase in 1-year mean ambient PM_{2.5} exposure (independent variable) in stratified and restricted subgroups. P values were calculated using linear regression models. Numbers in parentheses are 95% CIs.

* β coefficients represent the average difference in the magnitude of absolute native T1 mapping values in milliseconds (dependent variable) for every 1-μg/m³ increase in 1-year mean ambient PM_{2.5} exposure (independent variable) according to MRI unit field strength. P values were calculated using linear regression models.

Results

Patient Characteristics

An initial 506 eligible patients with DCM and 203 controls with normal cardiac MRI findings were identified. Fifteen patients were excluded, four due to LGE-based evidence of myocardial infarction, seven due to severe valvular insufficiency or stenosis on MRI scans, and four due to inability to assess T1 mapping images related to artifact (Fig 1). A total of 694 patients were included in the final study sample (age range, 18–88 years; mean age, 47 years ± 16 [SD]; 443 male), 493 with DCM (mean age, 48 years ± 16; 350 male) and 201 controls (mean age, 46 years ± 16; 93 male) (Table 1). The median of the 1-year mean daily ambient PM_{2.5} concentration was 7.7 μg/m³ (IQR: 7.2, 8.0). Cardiac MRI findings of patients are summarized in Table 2.

Association of Long-term PM_{2.5} Exposure with Myocardial Fibrosis

Overall, each 1-μg/m³ increase in 1-year mean ambient PM_{2.5} exposure was associated with a 0.38 higher native T1 z score (β coefficient: 0.38; 95% CI: 0.24, 0.51; *P* < .001) and helped explain 4.1% of the variance in native T1 in unadjusted analysis (Table 3, Fig 2). In a fully adjusted multivariable model, each 1-μg/m³ increase in 1-year mean PM_{2.5} exposure was associated with a 0.33 higher native T1 z score overall (adjusted β coefficient: 0.33; 95% CI: 0.19, 0.48; *P* < .001; adjusted *R*²: 0.120) (Fig 3). For absolute native T1 values, each 1-μg/m³ increase in 1-year mean PM_{2.5} exposure was associated with a 9.1-msec higher native T1 at 1.5 T (β coefficient for absolute T1 mapping values in milliseconds: 9.1; 95% CI: 2.04, 15.97; *P* = .01) and a 12.1-msec higher native T1 at 3 T (β coefficient for absolute T1 mapping values in milliseconds: 12.1; 95% CI: 5.74, 18.52; *P* < .001).

In adjusted multivariable models stratified by patient group (patients with DCM or controls with normal cardiac MRI), each 1-μg/m³ increase in 1-year mean PM_{2.5} exposure was associated with a higher native T1 z score of 0.30 in patients with DCM (adjusted β coefficient: 0.30; 95% CI: 0.13, 0.47; *P* < .001) and 0.27 in controls (adjusted β coefficient: 0.27; 95% CI: 0.04, 0.51; *P* = .02) (Table 3).

Association of Long-term PM_{2.5} Exposure with Other Indexes of Cardiac Remodeling

In individual multivariable models, after adjustment for potential confounders, each 1-μg/m³ increase in 1-year mean PM_{2.5} exposure was also associated with 40% higher odds of LGE (adjusted odds ratio: 1.4; 95% CI: 1.1, 1.7; *P* = .005), 3.6 mL/m² higher left ventricular end-diastolic volume indexed to body surface area (adjusted β coefficient: 3.6; 95% CI: 0.10, 7.2; *P* = .047), and 2.2% lower left ventricular ejection fraction (adjusted β coefficient: −2.2; 95% CI: −3.5, −0.80; *P* = .002) (Table 3). PM_{2.5} exposure was associated with higher native T2 z scores at univariable analysis (β coefficient: 0.10; 95% CI: 0.01, 0.19; *P* = .03). However, when adjusting for potential confounders in the multivariable model, there was no evidence of an association between PM_{2.5} exposure and T2 z scores (adjusted β coefficient: 0.07; 95% CI: −0.03, 0.17; *P* = .16).

In patients with DCM, each 1-μg/m³ increase in 1-year mean PM_{2.5} exposure was also associated with 25% higher odds of LGE in a multivariable model (adjusted odds ratio: 1.25; 95% CI: 1.01, 1.56; *P* = .04). PM_{2.5} exposure was associated with lower left ventricular ejection fraction values at univariable analysis in patients with DCM (β coefficient: −1.6; 95% CI: −3.1, −0.3; *P* = .045). However, when adjusting for potential confounders in the multivariable model, there was no evidence of this association (adjusted β coefficient: −1.2; 95% CI: −2.8, 0.3; *P* = .11). PM_{2.5} exposure was not associated with indexed left ventricular end-diastolic volume or T2 z scores in unadjusted or adjusted models in patients with DCM (adjusted β coefficient for indexed left ventricular end-diastolic volume: 2.6 [95% CI: −1.4, 6.6; *P* = .20]; adjusted β coefficient for the T2 z score: 0.05 [95% CI: −0.06, 0.16; *P* = .37]).

In patients with normal cardiac MRI findings, PM_{2.5} exposure was not associated with native T2 z score (β coefficient: 0.07; 95% CI: −0.01, 0.17; *P* = .48), left ventricular end-diastolic volume indexed to body surface area (β coefficient: −2.0; 95%

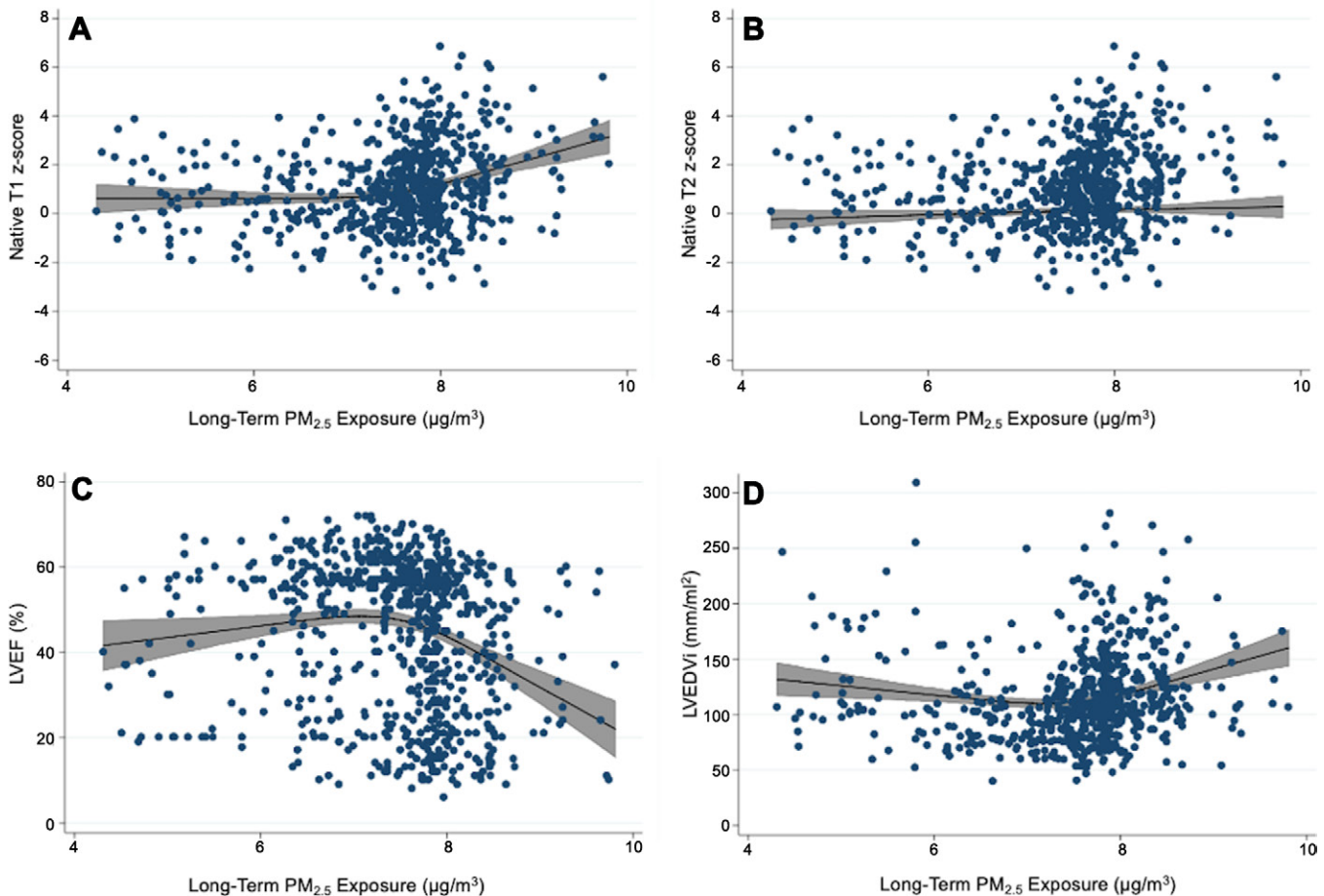


Figure 4: Scatterplots obtained with restricted cubic spline transformation (three knots) of 1-year mean fine particulate matter with 2.5- μm or smaller aerodynamic diameter ($\text{PM}_{2.5}$) exposure to investigate nonlinear relationships with cardiac MRI parameters in all patients, including (A) native T1 z score, (B) native T2 z score, (C) left ventricular ejection fraction (LVEF), and (D) left ventricular end-diastolic volume indexed to body surface area (LVEDVi). Regression lines are in black and 95% CIs in gray shading. Other than for left ventricular ejection fraction, there are no clear nonlinear relationships except for where there are few data points at extreme exposure values.

CI: $-5.4, 1.3$; $P = .24$), or left ventricular ejection fraction (β coefficient: -0.4 ; 95% CI: $-1.3, 0.5$; $P = .35$).

Age, Sex, Hypertension, Diabetes, and Smoking Effects of $\text{PM}_{2.5}$ Exposure on Myocardial Fibrosis

Overall, stratified models indicated largest effect sizes for the association of ambient $\text{PM}_{2.5}$ exposure with native T1 z scores in women (β coefficient: 0.49 ; 95% CI: $0.23, 0.76$; $P < .001$), in smokers (β coefficient: 0.43 ; 95% CI: $0.02, 0.84$; $P = .04$), and in patients with hypertension (β coefficient: 0.48 ; 95% CI: $0.16, 0.80$; $P = .004$) (Table 4). The effect estimate for the association of ambient $\text{PM}_{2.5}$ exposure with native T1 z scores was also large when restricted to patients with diabetes (β coefficient: 0.44 ; 95% CI: $-0.22, 1.10$; $P = .19$), although the association was not significant possibly due to the small sample size in the diabetes group. Effect sizes were similar between patients younger than 50 years (β coefficient: 0.31 ; 95% CI: $0.12, 0.50$; $P = .001$) and those aged 50 years or older (β coefficient: 0.29 ; 95% CI: $0.07, 0.52$; $P = .01$).

Sensitivity Analyses

Restricted cubic spline transformation of 1-year mean $\text{PM}_{2.5}$ exposure did not demonstrate alternate nonlinear concentration response relationships other than for left ventricular ejection

fraction (Fig 4). Using a linear spline term with one knot, each $1\text{-}\mu\text{g}/\text{m}^3$ increase in 1-year mean $\text{PM}_{2.5}$ exposure was associated with a 5.4% lower left ventricular ejection fraction (adjusted β coefficient: -5.4 ; 95% CI: $-9.0, -1.8$; $P = .003$) with $\text{PM}_{2.5}$ exposure of at least $7.7\text{ }\mu\text{g}/\text{m}^3$; however, there was no evidence of an association with $\text{PM}_{2.5}$ exposure less than $7.7\text{ }\mu\text{g}/\text{m}^3$ (adjusted β coefficient: -1.0 ; 95% CI: $-2.8, 0.7$; $P = .24$).

When the main analysis was restricted to individuals living within 10 km from a monitoring station (75.4%, 523 of 694 patients) and within 30 km from a monitoring station (93.5%, 649 of 694 patients), an association between long-term $\text{PM}_{2.5}$ exposure and native T1 z scores remained in adjusted models, with effect sizes similar to those in the full cohort (β coefficient for 10 km: 0.37 [95% CI: $0.19, 0.56$; $P < .001$]; β coefficient for 30 km: 0.38 [95% CI: $0.22, 0.54$; $P < .001$]).

Effect estimates for 1-year mean $\text{PM}_{2.5}$ exposure on native T1 z scores were similar to that of the overall cohort when restricted to MRI examinations performed before the COVID-19 pandemic (63.0%, 437 of 694 patients; β coefficient: 0.36 ; 95% CI: $0.17, 0.55$; $P < .001$) and when restricted to patients with 1-year mean $\text{PM}_{2.5}$ exposure below current Canadian Ambient Air Quality Standards (97.3%, 675 of 694 patients; β coefficient: 0.31 ; 95% CI: $0.16, 0.46$; $P < .001$). Key findings are summarized in Figure 5.

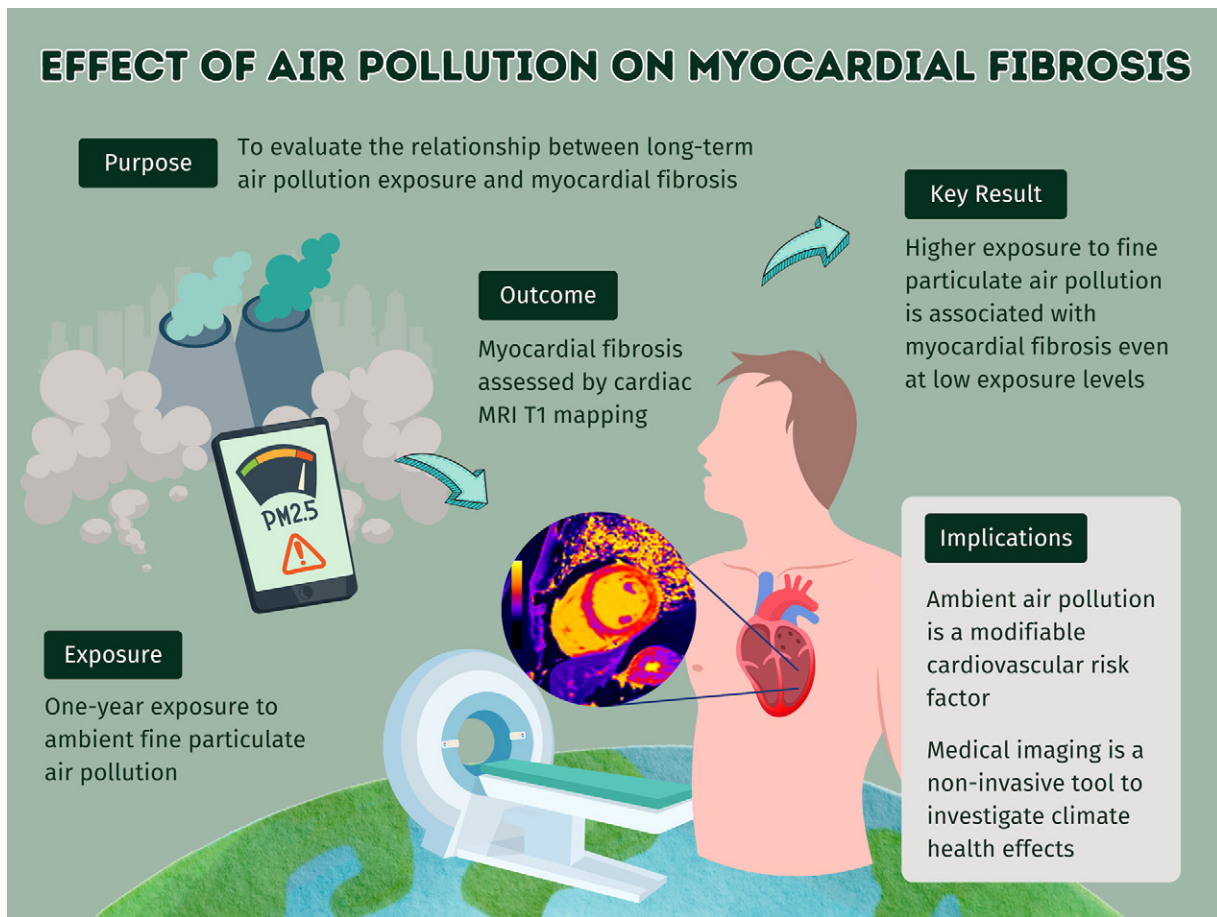


Figure 5: Diagram shows summary of study purpose, exposure, outcome, and key results. Higher long-term exposure to ambient fine particulate air pollution is associated with greater diffuse myocardial fibrosis at cardiac MRI native T1 mapping in patients with dilated cardiomyopathy and controls with normal MRI findings. PM_{2.5} = fine particulate matter with 2.5- μm or smaller aerodynamic diameter.

Discussion

Air pollution is associated with cardiovascular morbidity and mortality. However, the underlying pathophysiologic mechanisms are unclear. The relationship between long-term exposure to fine particulate matter with 2.5- μm or smaller aerodynamic diameter (PM_{2.5}) air pollution and myocardial fibrosis was evaluated in this retrospective study of 694 patients (493 with dilated cardiomyopathy and 201 controls with normal cardiac MRI findings). After adjusting for clinically relevant covariates, each 1- $\mu\text{g}/\text{m}^3$ increase in 1-year mean ambient PM_{2.5} exposure was associated with 0.30 higher native T1 z score in patients with dilated cardiomyopathy (β coefficient: 0.30; 95% CI: 0.13, 0.47; $P < .001$) and 0.27 higher native T1 z score in patients with normal cardiac MRI (β coefficient: 0.27; 95% CI: 0.04, 0.51; $P = .020$). Findings were robust at sensitivity analysis when restricted to MRI examinations performed before the COVID-19 pandemic and restricted to patients with 1-year mean PM_{2.5} exposure below current Canadian Ambient Air Quality Standards. Effects were largest in women (β coefficient: 0.49; 95% CI: 0.23, 0.76; $P < .001$), smokers (β coefficient: 0.43; 95% CI: 0.02, 0.84; $P = .038$), and patients with hypertension (β coefficient: 0.48; 95% CI: 0.16, 0.80; $P = .004$).

Our results are supported by those of a few prior studies that have demonstrated associations between air pollution exposure and cardiac MRI markers of ventricular remodeling (23,24,31). In an analysis of 3920 asymptomatic individuals free from

pre-existing cardiovascular disease in the UK Biobank population study, exposure to PM_{2.5} and nitrogen dioxide were associated with larger ventricular volumes (23). In patients with DCM, nitrogen dioxide exposure was associated with higher indexed left ventricular mass and lower left ventricular ejection fraction, with the largest effect in women (24). Notably, these studies did not assess markers of myocardial fibrosis. A strength of our study is a direct temporal relationship between assessed PM_{2.5} exposure and cardiac MRI, whereas other studies have estimated the effects of PM_{2.5} exposure based on more remote measurements (23).

Our findings are also concordant with prior animal models and autopsy studies and provide unique empirical data in human patients regarding the association between air pollution and myocardial fibrosis (13–15). Murine models have demonstrated that PM_{2.5} exposure induces myocardial fibrosis with a positive dose-response relationship, potentially mediated by transforming growth factor β signaling and activation of the renin-angiotensin system (13,14). In a postmortem study of 228 patients from Brazil, long-term exposure to air pollution estimated by means of black carbon accumulated in the lungs was associated with histopathologic extent of myocardial fibrosis, with the largest effects observed in patients with hypertension and a history of smoking (15).

In line with other studies, our results indicate that adverse effects of fine particulate air pollution on the heart are observed at exposures below current air quality guidelines, reinforcing

that there are no safe exposure limits (24). Our results bolster evidence that air pollution is a modifiable risk factor for cardiovascular disease (32). Air pollution contributes to health inequities both in terms of the level of exposure (with those of lower socioeconomic status likely to have higher exposure) and effect (with those that are already vulnerable being more biologically susceptible to the effects of pollutant exposure) (33). Our findings suggest that subgroups of patients may be more sensitive to long-term PM_{2.5} exposure, including women, those with hypertension, and those who smoke (15,24). Myocardial fibrosis is irreversible; therefore, it is imperative to implement measures to reduce exposure to long-term air pollution, especially in the most vulnerable patients (34–37).

Our study has several limitations. First, our findings may not be generalizable to all patients. We focused on patients with nonischemic DCM as the second most common cause of heart failure (21). Various underlying causes of non-ischemic DCM could impact MRI findings, although there are no data to suggest that DCM etiology impacts air pollution exposure. Similar effects were identified in a control group of patients with normal cardiac MRI findings, bolstering the conclusions. All imaging was performed at a single center, although patients were referred from across the province and had varying long-term exposure to PM_{2.5}. Exposures might have differed at earlier timepoints, particularly if patients moved. The 1-year mean PM_{2.5} exposure was evaluated as an indicator of long-term exposure similar to prior studies, given variability in air pollution estimates over longer periods (23,24). Second, although we adjusted multivariable models for a large number of potential confounders, there may be unknown and unmeasured confounders. This is a challenge in all observational studies. Notably, a randomized controlled trial of the effects of long-term PM_{2.5} exposure is not practical or ethical, and our findings remained robust in sensitivity analyses. Third, we only evaluated the effect of ambient (outdoor) PM_{2.5} and did not account for exposure to indoor PM_{2.5} or other air pollutants such as ozone and nitrogen dioxide. Air pollution is a complex mixture of both particulate and gaseous components. We focused on PM_{2.5} as the air pollutant most closely linked to detrimental health effects (38). Fourth, histologic confirmation of myocardial fibrosis was not available as endomyocardial biopsy is limited by invasiveness, the requirement for skilled operators, and the potential for sampling bias. Prior studies have demonstrated histologic validation that diffuse myocardial fibrosis in DCM is reliably assessed with native T1 mapping (18,19). Fifth, the study period overlaps with the COVID-19 pandemic, which impacted air pollution and cardiac imaging (28,39). However, we found similar effect estimates when the analysis was restricted to the pre-COVID-19 study period. Finally, our study identified associations between long-term ambient PM_{2.5} exposure and cardiac MRI markers of myocardial fibrosis but does not establish causality.

In conclusion, higher long-term exposure to ambient fine particulate air pollution is associated with greater diffuse myocardial fibrosis at cardiac MRI native T1 mapping in patients with dilated cardiomyopathy and healthy controls, indicating that myocardial fibrosis may be an underlying pathophysiologic mechanism by which air pollution leads to adverse cardiovascular health outcomes. Air pollution is ubiquitous, although the risks are not equal. Subgroups of patients may be more vulnerable, with exploratory analysis demonstrating largest effect

sizes in women, those with hypertension, and those who smoke. Public health measures are needed to reduce long-term air pollution exposure. In parallel, medical imaging can be used as a noninvasive tool to assess underlying mechanisms of climate and environmental disease (40,41). Future studies could adjust for additional variables, including patient occupation, and evaluate the association between longitudinal changes in air pollution exposure and MRI parameters.

Deputy Editor: Linda Moy

Scientific Editor: Kate Vilas

Author affiliations:

¹ University of Toronto, Department of Medical Imaging, Toronto, Ontario, Canada

² Joint Department of Medical Imaging, University Medical Imaging Toronto, University Health Network (UHN) and Sinai Health System (SHS), Toronto, Ontario, Canada

³ Department of Diagnostic Radiology, Queen's University, Kingston, Ontario, Canada

⁴ Department of Environmental Health, Harvard T. H. Chan School of Public Health, Boston, Mass

⁵ Department of Biostatistics, Harvard T. H. Chan School of Public Health, Boston, Mass

⁶ Division of Cardiology, Peter Munk Cardiac Centre, Ted Rogers Center for Centre for Heart Research, University Health Network (UHN), University of Toronto, Toronto, Ontario, Canada

⁷ Toronto General Hospital Research Institute, University Health Network (UHN), University of Toronto, 1 PMB-298, 585 University Ave, Toronto, ON M5G 2N2, Canada

Received October 24, 2024; revision requested November 21; final revision received May 16, 2025; accepted May 21.

Address correspondence to: K.H. (email: kate.hanneman@uhn.ca).

Funding: Authors declared no funding for this work.

Author contributions: Guarantor of integrity of entire study, **K.H.**; study concepts/study design or data acquisition or data analysis/interpretation, all authors; manuscript drafting or manuscript revision for important intellectual content, all authors; approval of final version of submitted manuscript, all authors; agrees to ensure any questions related to the work are appropriately resolved, all authors; literature research, **J.D.P., R.H., F.C., K.H.**; clinical studies, **C.D., R.H., H.R., F.C., K.H.**; statistical analysis, **S.D., R.C.N., P.T., K.H.**; and manuscript editing, **J.D.P., C.D., S.D., R.C.N., P.T., H.R., F.C., K.H.**

Disclosures of conflicts of interest: **J.D.P.** No relevant relationships. **C.D.** No relevant relationships. **S.D.** Grants from the National Institute on Aging (grant R01AG066793) and National Institute of Environmental Health Sciences (grant R01ES034373). **R.C.N.** Grants to institution from the U.S. National Institutes of Health, Health Effects Institute, and Harvard Climate Change Solutions Fund; support for presenting environmental health research from the Health Effects Institute. **R.H.** No relevant relationships. **P.T.** Speakers honoraria from AstraZeneca, Boehringer Ingelheim, and BeiGene. **H.R.** No relevant relationships. **F.C.** No relevant relationships. **K.H.** Payment or honoraria for lectures, presentations, speakers bureaus, manuscript writing or educational events from Sanofi; associate editor for *Radiology* and *Radiology: Cardiothoracic Imaging*.

References

- Landrigan PJ, Fuller R, Acosta NJR, et al. The Lancet Commission on pollution and health. *Lancet* 2018;391(10119):462–512.
- Orru H, Ebi KL, Forsberg B. The Interplay of Climate Change and Air Pollution on Health. *Curr Environ Health Rep* 2017;4(4):504–513.
- McKee H, Brown MJ, Kim HHR, et al. Planetary Health and Radiology: why We Should Care and What We Can Do. *Radiology* 2024;311(1):e240219.
- Brown M, Schoen JH, Gross J, Omary RA, Hanneman K. Climate Change and Radiology: impetus for Change and a Toolkit for Action. *Radiology* 2023;307(4):e230229.
- Rockall AG, Allen B, Brown MJ, et al. Sustainability in Radiology: position Paper and Call to Action from ACR, AOSR, ASR, CAR, CIR, ESR, ESRNM, ISR, IS3R, RANZCR, and RSNA. *Radiology* 2025;314(3):e250325.
- World Health Organization. Ambient (outdoor) air pollution. [https://www.who.int/news-room/fact-sheets/detail/ambient-\(outdoor\)-air-quality-and-health](https://www.who.int/news-room/fact-sheets/detail/ambient-(outdoor)-air-quality-and-health). Published 2022. Updated October 24, 2024. Accessed August 15, 2024.

7. Awe YA, Larsen BK, Sanchez-Triana E. The Global Health Cost of PM 2.5 Air Pollution: a Case for Action Beyond 2021. World Bank Group. <https://documents.worldbank.org/en/publication/documents-reports/document-detail/455211643691938459/the-global-health-cost-of-pm-2-5-air-pollution-a-case-for-action-beyond-2021>. Published June 16, 2022. Accessed August 15, 2024.
8. Krittanawong C, Qadeer YK, Hayes RB, et al. PM2.5 and cardiovascular diseases: state-of-the-Art review. *Int J Cardiol Cardiovasc Risk Prev* 2023;19:200217.
9. Gunasekaran S, Szava-Kovats A, Battey T, et al. Cardiovascular Imaging, Climate Change, and Environmental Sustainability. *Radiol Cardiothorac Imaging* 2024;6(3):e240135.
10. World Health Organization. Preventing disease through healthy environments: a global assessment of the burden of disease from environmental risks. <https://www.who.int/publications/i/item/9789241565196>. Published 2018. Accessed August 15, 2024.
11. World Heart Federation. World Heart Report 2024. <https://world-heart-federation.org/report2024/>. Published 2024. Accessed August 15, 2024.
12. Liu Y, Goodson JM, Zhang B, Chin MT. Air pollution and adverse cardiac remodeling: clinical effects and basic mechanisms. *Front Physiol* 2015;6:162.
13. Xing Q, Wu M, Xue Z, et al. Biochemical evidence of PM2.5 critical components for inducing myocardial fibrosis in vivo and in vitro. *Sci Total Environ* 2023;857(Pt 1):159258.
14. Zang X, Zhao J, Lu C. PM2.5 inducing myocardial fibrosis mediated by Ang II/ERK1/2/TGF- β 1 signaling pathway in mice model. *J Renin Angiotensin Aldosterone Syst* 2021;22(1):14703203211003786.
15. Takano APC, de André CDS, de Almeida R, Waked D, Veras MM, Saldiva PHN. Association of pulmonary black carbon accumulation with cardiac fibrosis in residents of Sao Paulo, Brazil. *Environ Res* 2024;248:118380.
16. Assomull RG, Prasad SK, Lyne J, et al. Cardiovascular magnetic resonance, fibrosis, and prognosis in dilated cardiomyopathy. *J Am Coll Cardiol* 2006;48(10):1977–1985.
17. Warnica W, Al-Arnawoot A, Stanimirovic A, et al. Clinical Impact of Cardiac MRI T1 and T2 Parametric Mapping in Patients with Suspected Cardiomyopathy. *Radiology* 2022;305(2):319–326.
18. Nakamori S, Dohi K, Ishida M, et al. Native T1 Mapping and Extracellular Volume Mapping for the Assessment of Diffuse Myocardial Fibrosis in Dilated Cardiomyopathy. *JACC Cardiovasc Imaging* 2018;11(1):48–59.
19. Iles LM, Ellims AH, Llewellyn H, et al. Histological validation of cardiac magnetic resonance analysis of regional and diffuse interstitial myocardial fibrosis. *Eur Heart J Cardiovasc Imaging* 2015;16(1):14–22.
20. Li S, Zhou D, Sirajuddin A, et al. T1 Mapping and Extracellular Volume Fraction in Dilated Cardiomyopathy A Prognosis Study. *JACC Cardiovasc Imaging* 2022;15(4):578–590.
21. Mandawat A, Chattranukulchai B, Mandawat A, et al. Progression of Myocardial Fibrosis in Nonischemic DCM and Association With Mortality and Heart Failure Outcomes. *JACC Cardiovasc Imaging* 2021;14(7):1338–1350.
22. Government of Ontario, Ministry of the Environment, Conservation and Parks. Air Pollutant Data. <https://www.airqualityontario.com/history/index.php>. Published 2023. Accessed February 1, 2024.
23. Aung N, Sanghvi MM, Zemrak F, et al. Association Between Ambient Air Pollution and Cardiac Morpho-Functional Phenotypes: insights From the UK Biobank Population Imaging Study. *Circulation* 2018;138(20):2175–2186.
24. Fecht D, Chadeau-Hyam M, Owen R, et al. Exposure to Elevated Nitrogen Dioxide Concentrations and Cardiac Remodeling in Patients With Dilated Cardiomyopathy. *J Card Fail* 2022;28(6):924–934.
25. Vassiliou VS, Heng EL, Gatehouse PD, et al. Magnetic resonance imaging phantoms for quality-control of myocardial T1 and ECV mapping: specific formulation, long-term stability and variation with heart rate and temperature. *J Cardiovasc Magn Reson* 2016;18(1):62.
26. Government of Canada. Historical Data. https://climate.weather.gc.ca/historical_data/search_historic_data_e.html. Published 2024. Updated March 20, 2025. Accessed March 1, 2024.
27. Fronza M, Thavendiranathan P, Chan V, et al. Myocardial Injury Pattern at MRI in COVID-19 Vaccine-Associated Myocarditis. *Radiology* 2022;304(3):553–562.
28. Hanneman K, Houbois C, Kei T, et al. Multimodality Cardiac Imaging, Cardiac Symptoms, and Clinical Outcomes in Patients Who Recovered from Mild COVID-19. *Radiology* 2023;308(1):e230767.
29. Hanneman K, Houbois C, Schoffel A, et al. Combined Cardiac Fluorodeoxyglucose-Positron Emission Tomography/Magnetic Resonance Imaging Assessment of Myocardial Injury in Patients Who Recently Recovered From COVID-19. *JAMA Cardiol* 2022;7(3):298–308.
30. Canadian Council of Ministers of the Environment. Canadian Ambient Air Quality Standards. <https://ccme.ca/en/air-quality-report>. Published 2020. Accessed September 1, 2024.
31. Aaron CP, Chervona Y, Kawut SM, et al. Particulate Matter Exposure and Cardiopulmonary Differences in the Multi-Ethnic Study of Atherosclerosis. *Environ Health Perspect* 2016;124(8):1166–1173.
32. Brauer M, Casadei B, Harrington RA, et al; WHF Air Pollution Expert Group. Taking a Stand Against Air Pollution—The Impact on Cardiovascular Disease. *J Am Coll Cardiol* 2021;77(13):1684–1688.
33. Hajat A, MacLehose RF, Rosofsky A, Walker KD, Clougherty JE. Confounding by Socioeconomic Status in Epidemiological Studies of Air Pollution and Health: challenges and Opportunities. *Environ Health Perspect* 2021;129(6):65001.
34. Bing R, Dweck MR. Myocardial fibrosis: why image, how to image and clinical implications. *Heart* 2019;105(23):1832–1840.
35. Taboun O, DesRoche C, Hanneman K. Imperative for a health-centred focus on climate change in radiology. *J Med Imaging Radiat Oncol* 2024.
36. Hanneman K, Taboun O, Kirpalani A, et al. Increased Emergency Department Medical Imaging: association with Short-Term Exposures to Ambient Heat and Particulate Air Pollution. *Radiology* 2024;313(2):e241624.
37. Chaban YV, Vosschenrich J, McKee H, et al. Environmental Sustainability and MRI: challenges, Opportunities, and a Call for Action. *J Magn Reson Imaging* 2024;59(4):1149–1167.
38. Wei Y, Coull B, Koutrakis P, et al. Assessing additive effects of air pollutants on mortality rate in Massachusetts. *Environ Health* 2021;20(1):19.
39. Venter ZS, Aunan K, Chowdhury S, Lelieveld J. COVID-19 lockdowns cause global air pollution declines. *Proc Natl Acad Sci U S A* 2020;117(32):18984–18990.
40. Castillo F, Taboun O, Farag Alla J, Yankova K, Hanneman K. Imaging Climate-Related Environmental Exposures: impact and Opportunity. *Can Assoc Radiol J* 2025;8465371251322762.
41. DesRoche C, Castillo F, Sharma S, et al. Climate resilient and environmentally sustainable radiology: a framework for implementation. *Radiology Advances* 2025;2(2).